JURNAL PENELITIAN KEHUTANAN WALLACEA
eISSN 2407-7860; pISSN 2302-299X
https://doi.org/10.24259/jpkwallacea.v14i2.48907

Short communication

Ecological Disaster in Northern Sumatra: How Extreme Rainfall and Land-Cover Disturbance Triggered Widespread Flash Flooding

Nasri[1*], Munajat Nursaputra[2*], Abdur Rahman Arif[3], Risye Dwiyani[4], Lady Chania[5], Ida Bagus Oka Agastya[4], Dian Adhetya Arif[6]

[1]Forest Conservation Department, Hasanuddin University, Makassar, Indonesia
[2]Forestry Department, Hasanuddin University, Makassar, Indonesia
[3]Chemistry Department, Hasanuddin University, Makassar, Indonesia
[4]U-INSPIRE Indonesia, Bogor, West Java, Indonesia
[5]The United Graduated School of Agricultural Sciences, Ehime University, Matsuyama, Japan
[6]Remote Sensing & GIS Department, Universitas Negeri Padang, Padang, Indonesia
* Corresponding authors: nasri@unhas.ac.id, munajatnursaputra@unhas.ac.id

Received 11 December 2025;
Accepted 29 December 2025;
Published online 31 December 2025

Citation: Nasri, Nursaputra, M., Arif, A.R., Dwiyani, R., Chania, L., Agastya, I.B.O., & Arif, D.A. 2025. Ecological Disaster in Northern Sumatra: How Extreme Rainfall and Land-Cover Disturbance Triggered Widespread Flash Flooding. JPK Wallacea, Vol. 14 No. 2 pp. 111-121

Abstract. In November 2025, Northern Sumatra experienced one of the most extreme flood disasters in recent history, triggered by a rare combination of sustained high-intensity rainfall and long-term land-cover disturbance. Using satellite-based rainfall estimates, historical rainfall records, and land-cover change analysis, this study examines the spatial and temporal dynamics of the event. The rainfall produced over 950 mm within four days, with daily accumulation exceeding 390 mm and hourly peaks surpassing 40 mm/hr. Statistical analysis using the Generalized Extreme Value (GEV) distribution estimated a return period of approximately 192 years for the daily maximum. Land-cover analysis revealed extensive deforestation between 1990 and 2024, including in designated protection and conservation forest zones. Flood impacts were concentrated in watersheds with high forest loss and recent land disturbance, particularly in Aceh and North Sumatra. This study highlights how compounding hydroclimatic extremes and upstream land degradation can significantly amplify flood risk. The findings underscore the importance of integrating forest conservation and multi-day rainfall indicators into regional flood risk assessments and early warning systems.

Keywords: Deforestation, ecological disaster, extreme rainfall, flash flood, land-cover change, Northern Sumatra

INTRODUCTION

Flash floods are among the most destructive hydrometeorological hazards in tropical regions, often triggered by intense rainfall and exacerbated by upstream land-cover change (Jothityangkoon et al., 2013; Abdulkareem et al., 2018). In Indonesia, flood disasters have increased in frequency and severity over the past two decades, with recent studies linking their impacts to deforestation, unregulated land conversion, and limited early warning capacity (Widodo et al., 2021; Golar et al., 2024). The November 2025 disaster in Aceh, North Sumatra, and West Sumatra, a region hereafter referred to as Northern Sumatra, represents one of the most extreme and deadly events in recent memory, affecting multiple watersheds and resulting in significant loss of life and infrastructure damage.

Compound rainfall events, defined by both high hourly intensity and sustained multi-day accumulation, are increasingly recognized as critical drivers of extreme flood hazards under a changing climate (Zscheischler et al., 2018; AghaKouchak et al., 2020; Gori et al., 2020). Yet, there remains a limited

understanding of how such rainfall structures interact with long-term landscape degradation to amplify disaster impacts, particularly in forest-rich yet vulnerable regions like Northern Sumatra.

This study presents an integrated analysis of the November 2025 flood event by combining satellite-derived rainfall data, 25-year rainfall records, historical land-cover change, and flood impact mapping. The findings demonstrate how the intersection of hydroclimatic extremes and upstream deforestation intensified flood severity and exposure.

MATERIAL AND METHODS

This study integrates satellite-based rainfall observations, historical rainfall records, land cover datasets, and flood impact data to examine the November 2025 flood event in the primary disaster-affected areas of Northern Sumatra, with a focus on the co-occurance of extreme rainfall and long-term land cover change.

Rainfall analysis and extreme value statistics

Hourly rainfall data were obtained from the Integrated Multi-satellite Retrievals for GPM (IMERG Final Run, V07) at 0.1° resolution for 22–28 November 2025. Key rainfall metrics were computed to map spatial variation in intensity and accumulation. To contextualize the event, an hourly IMERG rainfall time series from 2000 to 2025 was aggregated to daily totals, and an annual maximum series (AMS) was extracted. To estimate the return period and annual exceedance probability of the 2025 daily maximum, the Generalized Extreme Value (GEV) distribution was fitted to the AMS using the genextreme function from the SciPy library in Python. Model performance and goodness of fit were evaluated using probability–probability (P–P) plots, quantile–quantile (Q–Q) plots, and probability density function (PDF) curves.

Land cover change and deforestation analysis

Land cover maps for 1990 and 2024 were sourced from Indonesia's Ministry of Environment and Forestry, based on Landsat, and analyzed using QGIS 3.34 Prizren. The maps were clipped to the administrative boundaries of Aceh, North Sumatra, and West Sumatra provinces, and land cover classes were grouped into forest and non-forest categories. Forest loss was defined as any transition from forest classes to non-forest classes, including conversion to plantations, dryland agriculture, mining areas, settlements, and other land categories. Total forest loss and dominant conversion pathways between 1990 and 2024 were quantified and summarized at the provincial level. To assess deforestation within legally designated forest zones, the land-cover maps were overlaid with Indonesia’s official forest classification, consisting of conservation forest, protection forest, and production forest. This overlay was used to estimate forest loss by forest function and province, thereby indicating the extent to which deforestation occurred inside designated forest areas.

Flood impacts and critical watershed conditions

Flood impacts were characterized using spatial data on flood casualties (fatalities and missing persons), compiled up to 8 December 2025 from official reports issued by the Indonesian National Agency for Disaster Management (BNPB, 2025), and complemented with systematically screened online news reports to fill data gaps and verify event locations. Each casualty record was geocoded to the affected administrative unit and then linked to the corresponding watershed through spatial overlay with watershed boundaries. This procedure was used to identify watersheds with the highest numbers of casualties and to flag hydrologically critical. For selected critical watersheds, Sentinel 2 imagery was visually analyzed to assess upstream land cover disturbance. Cloud-free median image composites were used to represent conditions approximately five years before the flood (1 January to 31 December 2020), immediately before the November 2025 event (1 October to 20 November 2025), and shortly after the flood (25 to 30 November 2025). Cloud-free scenes acquired approximately five years before the event, immediately before November 2025, and in the months following the flood were used as a temporal image series. Comparison of these images was used to identify the expansion of disturbed land, plantation, open areas, and the emergence of surface scars consistent with landslides or severe erosion in headwater regions.

RESULTS

Spatial and temporal dynamics of the November 2025 rainfall

The rainfall event between 25 and 27 November 2025 showed exceptionally high hourly intensities and multi-day accumulation across Northern Sumatra. Maximum hourly intensity exceeded 50 mm/hr in the northern part of Aceh Province, particularly in upstream watersheds near the North Sumatra border (Figure 1B), while mean intensities reached up to 9 mm/hr over a wide area (Figure 1A). Three-day totals surpassed 800 mm in northern Aceh, with more than 500 mm extending into parts of North Sumatra, while West Sumatra experienced lower but still substantial multi-day rainfall totals (Figure 1C). These regions experienced sustained high rainfall for three consecutive days, substantially increasing hydrological pressure in downstream watersheds.

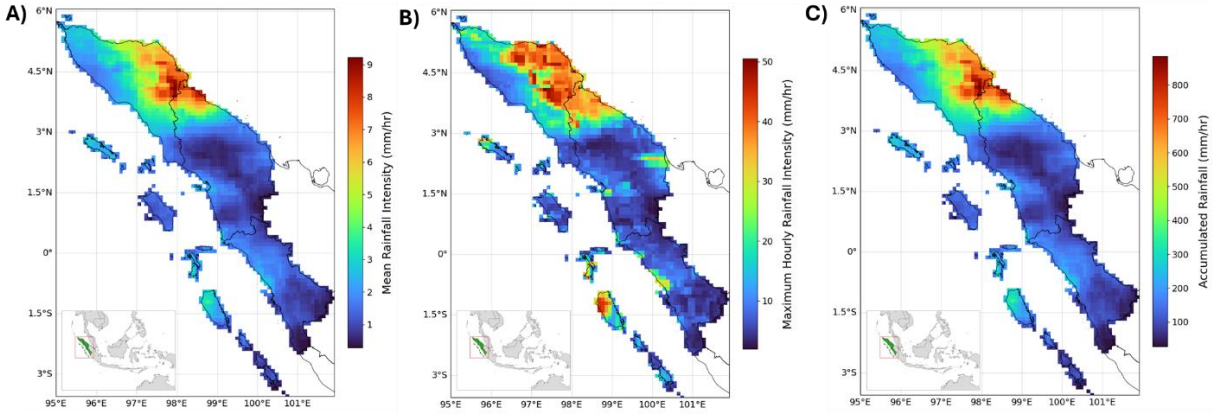

Figure 1. Spatial distribution of rainfall characteristics in Northern Sumatra during 25–27 November 2025: (A) Mean rainfall intensity (mm/hr), (B) Maximum hourly rainfall intensity (mm/hr), and (C) Total accumulated rainfall (mm).

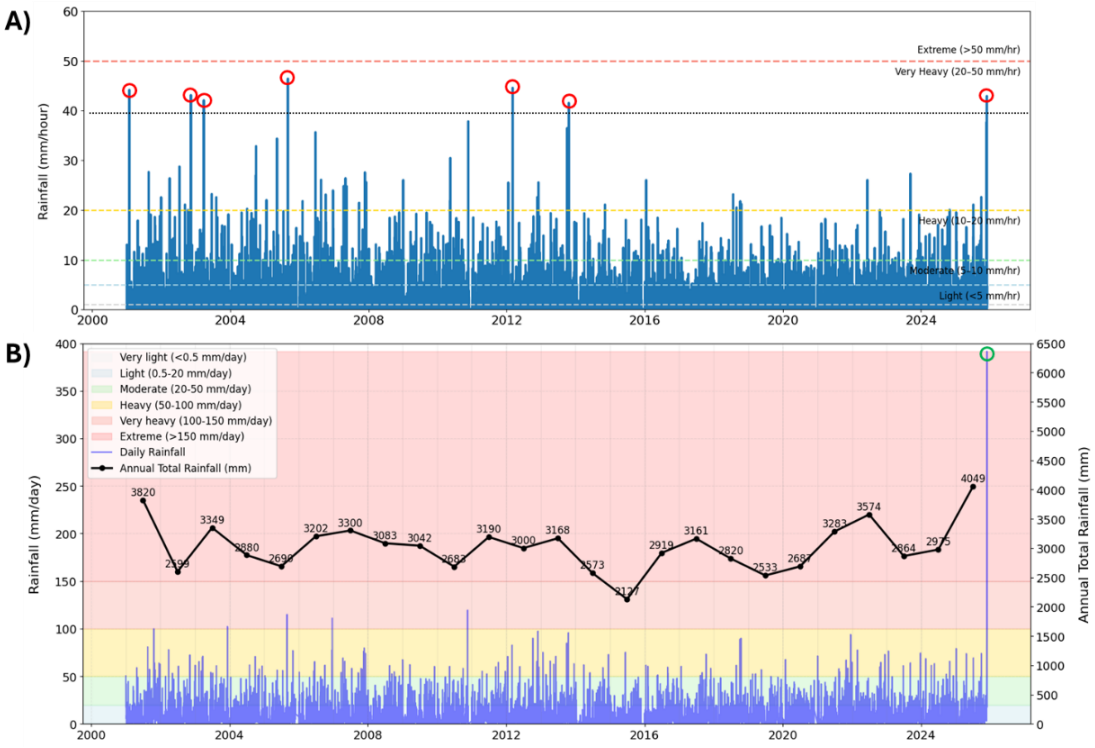

Figure 2. Time series of rainfall intensity in Northern Sumatra from 2000 to 2025. (A) Hourly rainfall intensity (mm/hr), where seven extreme events exceeding 40 mm/hr are marked with red circles. (B) Daily rainfall (bars, mm/day) and annual total rainfall (black line, mm/year), overlaid on color-coded rainfall intensity categories. The green circle marks the 26 November 2025 event, with a daily total of approximately 390 mm.

Historical analysis (2000-2025) shows that rainfall bursts above 40 mm/hr occurred seven times (Figure 2A). During the period 2000–2024, six such events occurred; however, these were isolated, short-lived, typically limited to one or two hours, and did not produce extreme daily totals. In contrast, the November 2025 event combined persistent high hourly intensities with exceptional volume, with 26 November 2025 reaching approximately 390 mm/day, the highest single-day total in the 25-year record (Figure 2B). The 2025 annual rainfall also exceeded 4,000 mm, setting the highest total in the observation period.

Comparison with historical extreme events

Hourly GPM data show that the 24–27 November 2025 event was a long-duration and high-impact rainfall episode, with 957.21 mm accumulated over four days (Figure 3). The event began with heavy rain at 20:00 on 24 November and reached the first extreme burst (>20 mm/hr) by 07:00 the next day. In total, 18 hours recorded extreme rainfall and 11 hours recorded heavy rainfall (10–20 mm/hr), together contributing over 70% of the total, with extreme intensity alone accounting for 56.7% (542.59 mm). The peak hour (42.91 mm/hr) occurred at 11:00 on 26 November, which alone contributed approximately 390 mm. The steep rise in the cumulative rainfall curve between 25-26 November indicates concentrated phase of intense and sustained rainfall.

AMS analysis using daily rainfall (2000-2025) fitted with GEV distribution shows a strong statistical fit, with p-value of 0.981 and R^2 of 0.720 (Q–Q) and 0.987 (P–P) (Figure 4). The 2025 event, with a daily total of 391.42 mm, corresponds to a return period of approximately 192 years and an annual exceedance probability (AEP) of 0.0052 (0.5% chance/year). In contrast, other historical maxima had return periods under 10 years (AEP > 0.1). The return value and PDF plot highlight the rarity of the 2025 event, which lies far in the upper tail of the fitted distribution, with modeled density dropping sharply beyond 300 mm. The Q–Q and P–P plots confirm the robustness of the GEV model for capturing extreme rainfall behaviour in the region.

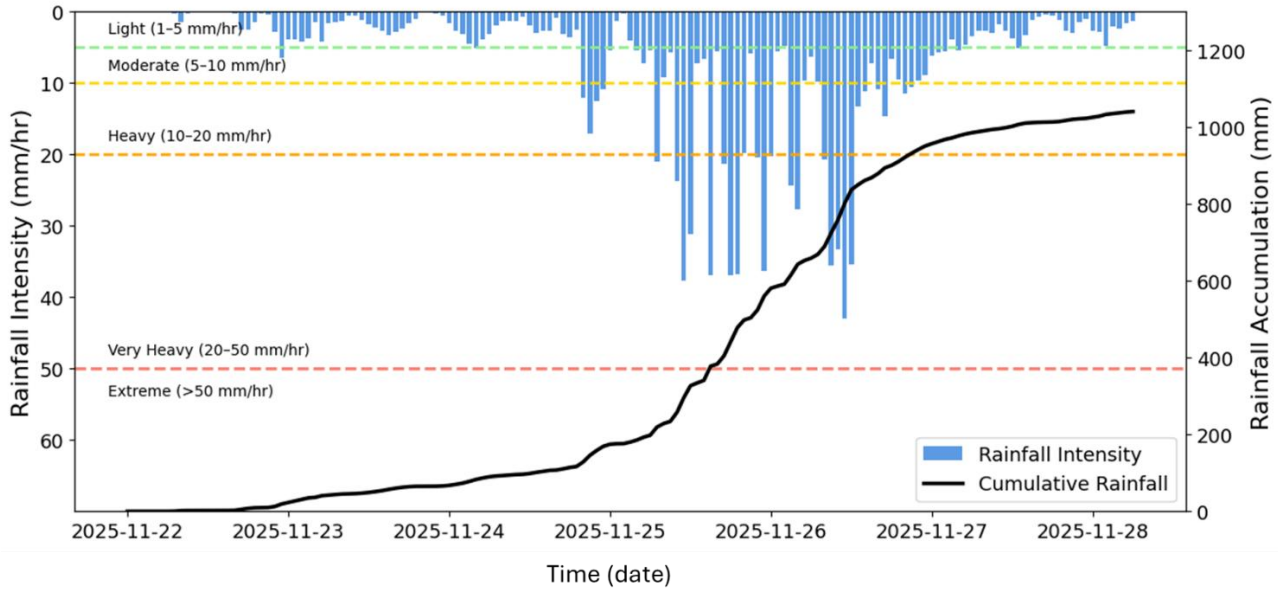

Figure 3. Hourly rainfall intensity and cumulative rainfall in Northern Sumatra from 22 to 28 November 2025. Hourly rainfall (blue bars) and cumulative total (black line) are derived from GPM satellite data. Dashed horizontal lines indicate rainfall intensity categories.

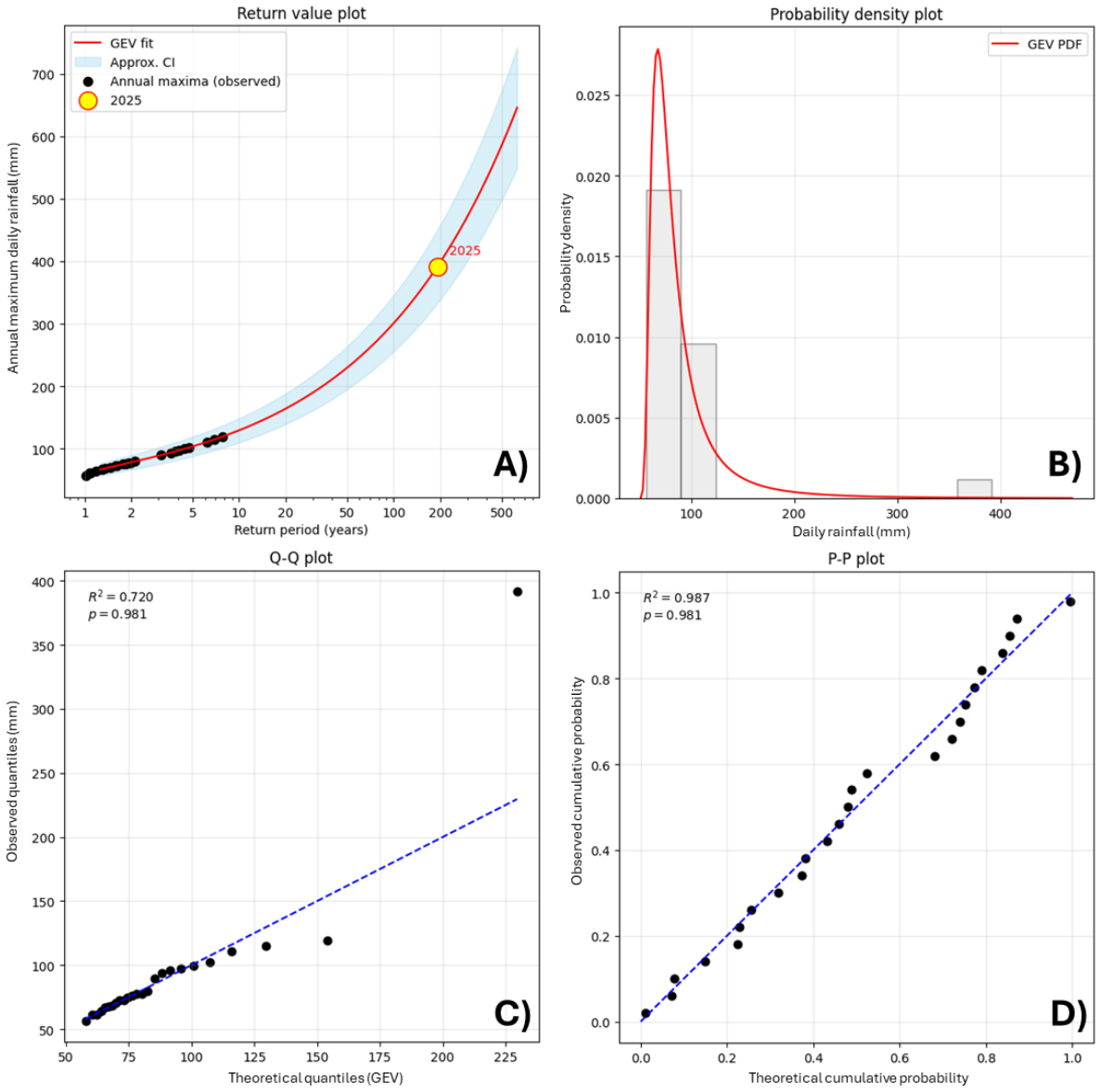

Figure 4. Statistical analysis of annual maximum daily rainfall in Northern Sumatra based on the GEV distribution. (A) Return value plot showing fitted GEV curve with confidence interval (shaded blue); the 2025 event (yellow point) corresponds to a return period of approximately 192 years. (B) Probability density function (PDF). (C) Quantile–Quantile (Q–Q). (D) Probability–Probability (P–P).

Long-term land-cover change and deforestation in Northern Sumatra

Land-cover maps and time series show major forest loss across Northern Sumatra between 1990 and 2024, especially in Aceh, West Sumatra, and North Sumatra, provinces severely impacted by the 2025 floods (Figure 5A–B). During this period, 36.7% of Aceh's forests were converted to non-forest uses, compared to 17.1% in West Sumatra and 10.5% in North Sumatra. In contrast, afforestation remained limited, reaching only about 1.2%, 2.6%, and 7.5% of provincial area in Aceh, West Sumatra, and North Sumatra, respectively (Figure 5E). Deforestation resulted from multiple land-use conversions, including plantations, dryland agriculture, mining areas, settlements, and other land categories (Figure 5C, D). In Aceh, 70.5% of forest loss was due to agriculture and 29.2% to plantations. West Sumatra and North Sumatra showed more balanced shares between the two drivers.

Analysis of forest areas shows that deforestation also occurred within official forest function zones, including conservation, protection, and production forests (Figure 6A). Forest zones covered 69% of Aceh, 56% of West Sumatra, and 36% of North Sumatra (Fig. 6B), showing that even conservation and protection

forests faced land-cover change. Provincial patterns of deforestation within these zones vary (Figure 6C). In Aceh, 73% of deforestation occurred inside conservation (32.6%) and protected forests (40.7%). In West Sumatra, half of forest loss occurred in the other land users with the remainder split across forest functions. In North Sumatra, forest loss was concentrated in production forests (49.2%) and other land uses (34.4%).

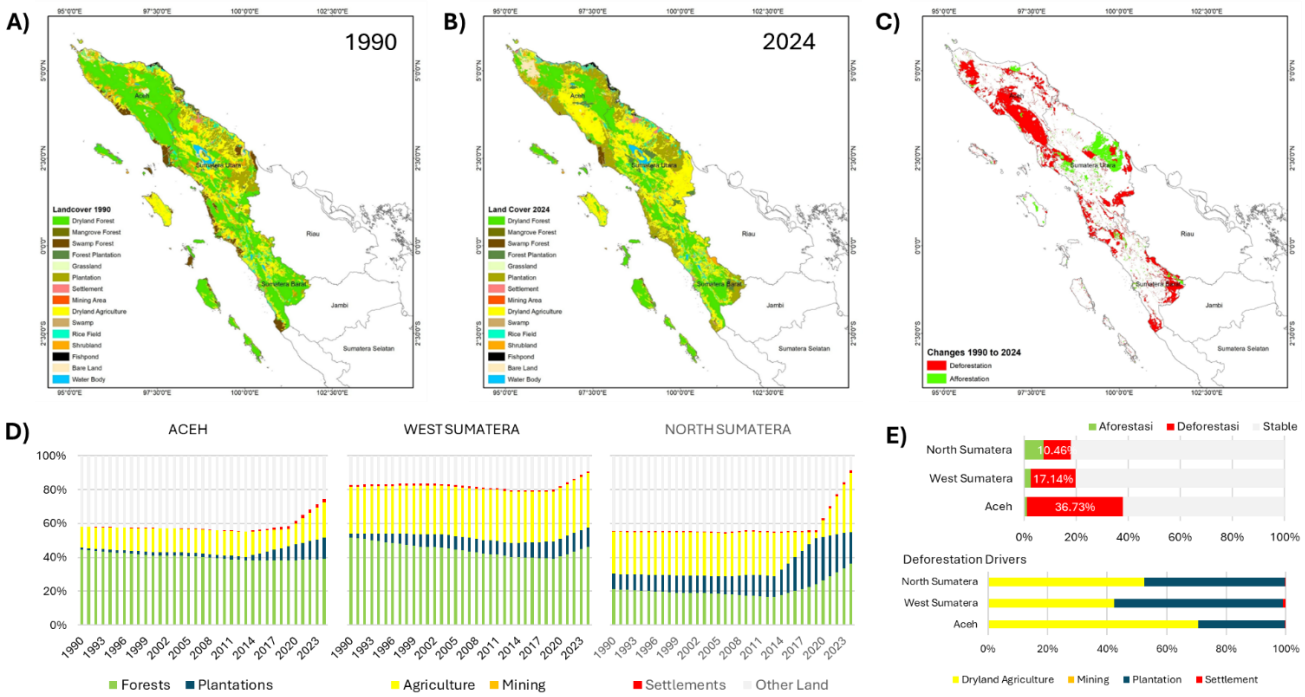

Figure 5. Land-cover changes and deforestation in Northern Sumatra between 1990 and 2024. (A) Land-cover map for 1990. (B) Land-cover map for 2024. (C) Spatial distribution of land-cover change from 1990 to 2024, showing areas of deforestation (red) and afforestation (green). (D) Time series of land-cover composition by province. (E) Summary of deforestation, afforestation, and main land-cover conversion drivers by province.

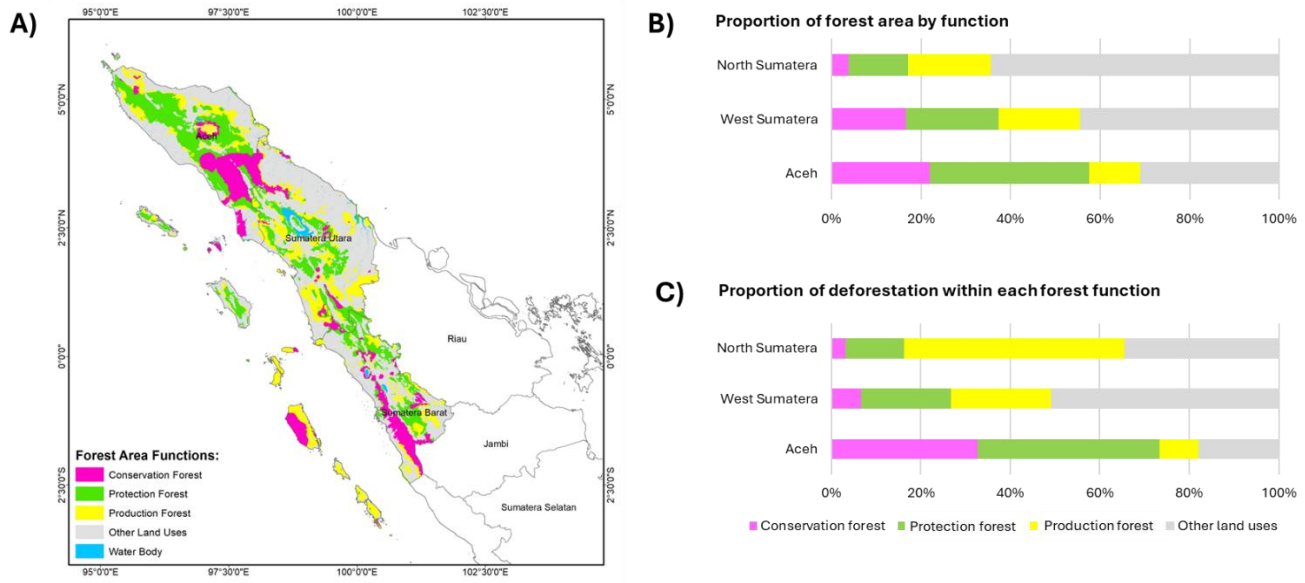

Figure 6. Deforestation inside designated forest areas in Northern Sumatra. (A) Spatial distribution of forest area functions. (B) Proportion of total functional forest area in each province. (C) Proportion of deforestation occurring within each forest function category for the three provinces from 1990 to 2024.

Critical watersheds and flood impact zones

Flood-related casualties during the November 2025 event were concentrated in specific watersheds across Northern Sumatra (Figure 7). The largest clusters of deaths and missing persons were associated with rivers draining to the northern and western coasts. In Aceh, high-impact locations included the Jambo Aye, Kluet, Krueng Aceh, Krueng Baro, Krueng Beuracan, Krueng Geukueh, Krueng Mane, Krueng Pasee, Krueng Keureutou, Krueng Langsa, Krueng Tripa, Peusangan, Tamiang, Woyla, and Singkil watersheds. In North Sumatra, casualties were concentrated in the Batang Serangan, Belumai, Deli, Batang Gadis, Batang Toru, Kolang, Mola, Sibuluan, Sibundong, and Susua watersheds. In West Sumatra, reported impacts were linked to the Anai, Kuranji, Masang Kiri, and Pasaman watersheds. These watersheds, highlighted in Figure 8 insets, represent a small number of critical watersheds accounting for a disproportionate share of reported deaths and missing persons.

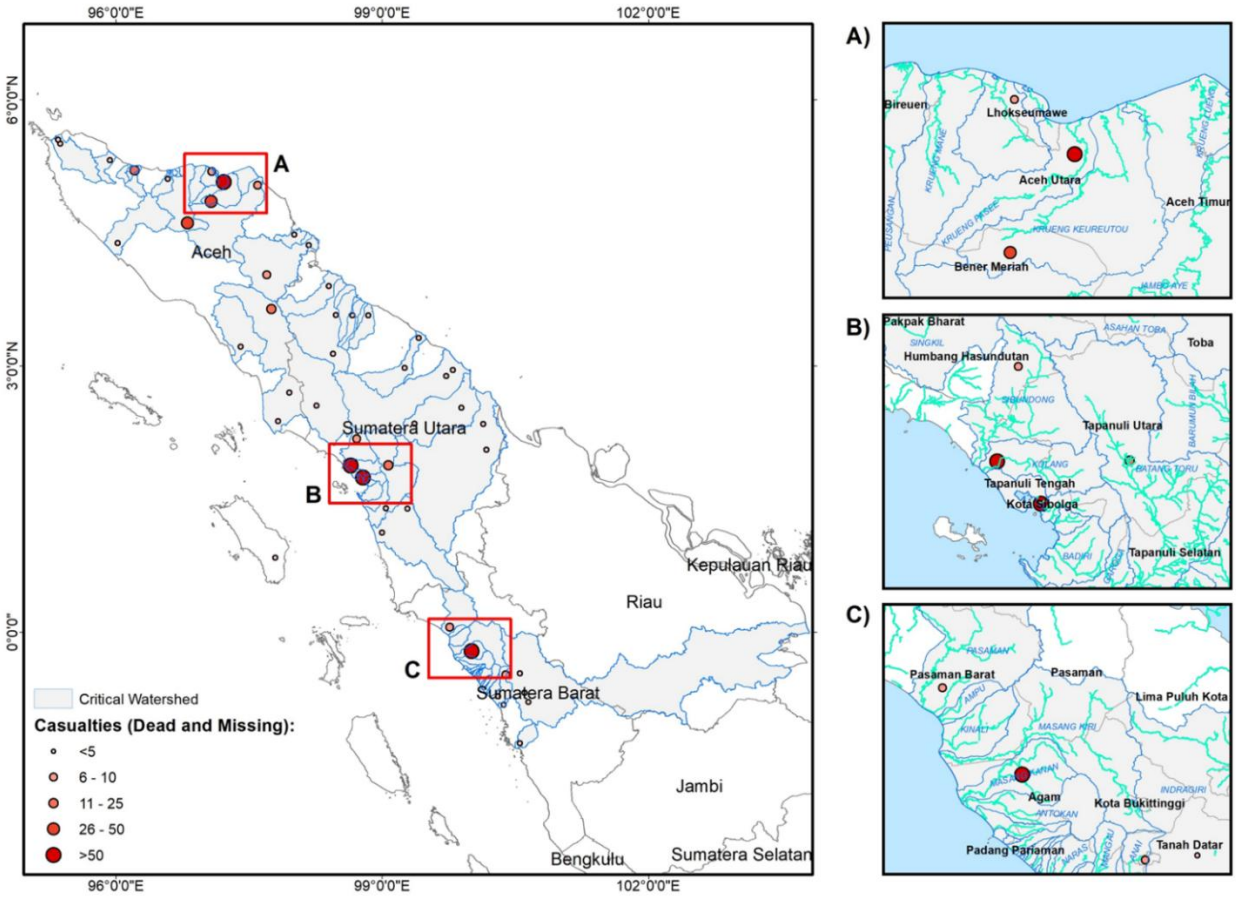

Figure 7. Spatial distribution of critical watersheds in Northern Sumatra and recorded casualties (dead and missing) associated with the November 2025 flooding. Circle sizes represent casualty severity per location, based on reports compiled and updated through 8 December 2025. Insets A–C show zoomed views of high-impact watersheds in Aceh, North Sumatra, and West Sumatra.

Although numerous watersheds in Northern Sumatra were affected, Figure 8 highlights two illustrative cases from Aceh to demonstrate the combined effects of upstream land-cover disturbance and downstream inundation patterns. Comparisons from five years before, immediately prior to, and after the flood show persistent inundation along river corridors in North Aceh and expanding disturbed land in the upper catchments, particularly around Krueng Mane and Krueng Pasee. These examples reflect typical patterns observed across other impacted watersheds. A similar situation is visible in Padang City, West Sumatra, where settlement expansion has pushed built-up areas into high-risk flood zones, increasing exposure to severe inundation (Figure 9). Post-flood imagery shows that these newly developed areas within known hazard zones experienced some of the worst flooding.

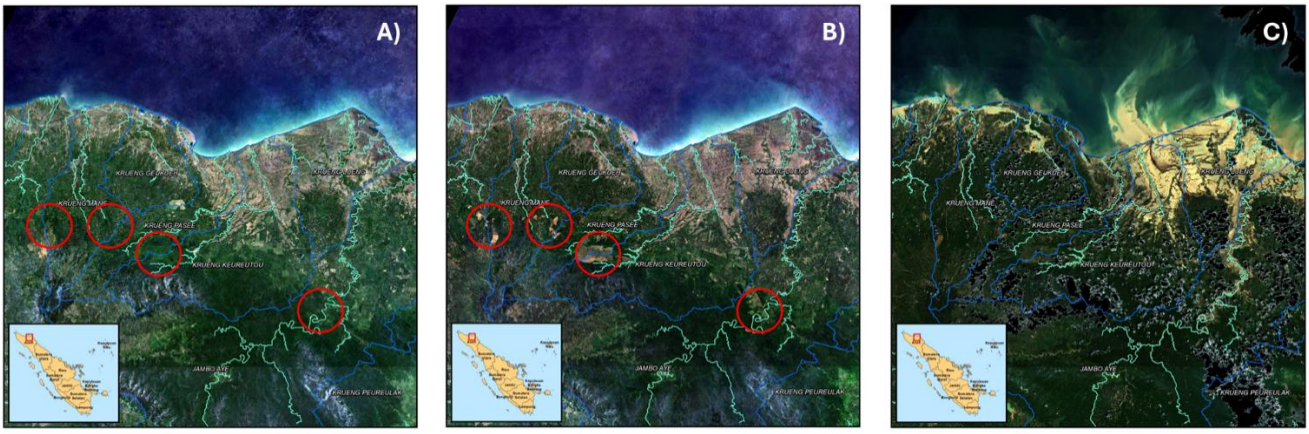

Figure 8. Time series of Sentinel-2 imagery showing land-cover changes and flood inundation in the upstream areas of critical watersheds in Aceh: (A) Five years prior to the flood; (B) Immediately before the November 2025 event; (C) After the flood. Highlighted areas show affected upper-catchment and floodplain zones such as those observed in Krueng Mane and Krueng Pasee.

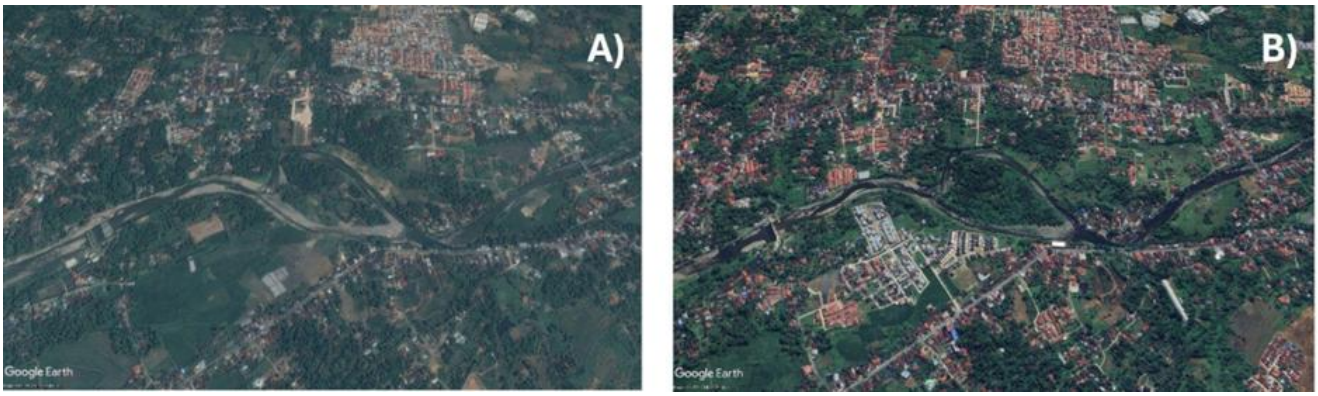

Figure 9. Comparison of flood-prone areas and settlement development: (A) The 2014 satellite-derived image indicates flood-prone zones with limited built-up areas; (B) The 2025 image shows substantial expansion of urban settlements into previously vacant flood-prone zones.

DISCUSSION

The 2025 flash flood disaster in Northern Sumatra was driven by a rare combination of meteorological extremes and long-term landscape degradation. The rainfall event over 24–27 November featured both high hourly intensities and exceptional multi-day totals, with 26 November alone reaching nearly 390 mm, a magnitude corresponding to a 192-year return period. While intense hourly rainfall (>40 mm hr^{-1}) has occurred in previous years, the prolonged duration and cumulative volume of this event distinguish it as a rare compound extreme in the regional climatology. The temporal and spatial coherence was likely amplified by convective organization linked to a mesoscale convective system (MCS) enhanced by the presence of Tropical Cyclone Senyar, consistent with previous findings on the role of MCS in tropical cyclone intensification (Goyal et al., 2016; Silpamol et al., 2025). Tropical cyclones have been shown to increase deep convection and moisture flux in equatorial zones, especially in mountainous terrain where orographic lifting intensifies rainfall (Chen et al. 2010, Houze, 2012; Huang et al., 2020). The resulting focused rainfall in northern Aceh and North Sumatra demonstrates how regional-scale meteorology can interact with local topography to produce devastating outcomes (Daly et al., 2009; Dimri, 2009; Cao et al., 2020). This interaction defines the hazard component of the disaster, but the resulting impacts were ultimately shaped by a broader risk landscape influenced by human–environment interactions.

However, meteorological triggers alone cannot fully explain the scale of the disaster. Land-cover data between 1990 and 2024 reveal massive deforestation, primarily due to the expansion of plantations, dryland agriculture, and settlements. Critically, much of this deforestation occurred within designated forest

areas, including protection and conservation zones. Such large-scale forest loss has been widely linked to increased runoff, reduced infiltration, and decreased slope stability, thereby amplifying flood and landslide risks (Dolidon et al., 2009; Buthurst et al., 2010; Mantero et al., 2020). Importantly, several watersheds in West Sumatra also experienced severe impacts despite receiving lower rainfall totals than Aceh, indicating that landscape degradation, rather than rainfall magnitude alone, played a decisive role in shaping downstream damage.

The spatial concentration of casualties within specific watersheds underscores the strong influence of landscape conditions on disaster impacts. In Aceh and North Sumatra, fatalities were clustered in basins exposed to both intense rainfall and substantial forest disturbance, with Sentinel-2 imagery from the Krueng Mane and Krueng Pasee watersheds showing expanding plantations and open areas prior to the event, followed by surface scarring and erosion consistent with landslides. These signals point to compounded vulnerability, where degraded upstream landscapes accelerate hydrological response and intensify downstream impacts (Nepal et al., 2014; van Vliet et al. 2023). Settlement dynamics further heightened exposure: rapid urbanization has pushed residential and commercial development into flood-prone zones (Alves et al., 2023), as seen in Padang City where limited developable land and steep terrain have driven settlement growth into high-risk corridors, and in Palembayan, Agam Regency, where rural communities occupy narrow hilly valleys highly susceptible to flash floods and landslides (BNPB, 2025). Together, these patterns demonstrate how environmental degradation and spatial development pressures amplify exposure and make vulnerability as consequential as the meteorological hazard itself.

Taken together, the disaster did not arise from a single dominant driver but from the convergence of hydroclimatic extremes, extensive land-cover change, high population exposure along river corridors, and limitations in preparedness and early warning capacity. This complexity reflects the broader view of disaster risk as the interaction of hazard, exposure, and vulnerability, shaped by institutional and community capacity to respond and recover (Cutter et al., 2003; Wisner et al., 2004; UNDRR, 2019). The event exemplifies an emerging class of ecological disasters in which extreme hydroclimatic forcing intersects with land degradation, highlighting the need for integrated watershed management and strengthened forest governance, including deforestation moratoria in critical basins. Given that deforestation persists even within protected areas, recovery will require sustained efforts that incorporate local wisdom and traditional ecological knowledge (Basuki et al., 2022). In parallel, early warning systems must evolve beyond short-term intensity thresholds by integrating multi-day rainfall accumulation, land-cover information, and real-time indicators of watershed vulnerability, and potential flow obstructions caused by wood debris accumulation to better anticipate future extremes.

ACKNOWLEDGEMENT

This research was conducted without external support or specific contributions requiring acknowledgement.

AUTHOR CONTRIBUTIONS

Conceptualization and designed the experiments: NN and MN; Methodology: NN and MN; Performed the experiments and analysed the data: MN; Visualization: NN and MN; Writing – original draft: NN and MN; Writing – review and editing: NN, MN, AR, RD, LC, IB, and DA. All the authors have read and agreed to the published version of the manuscript.

CONFLICTS OF INTEREST

The authors declare that there are no conflicts of interest and no external funding was received for this study.

REFERENCES

Abdulkareem, J.H., Sulaiman, W.N.A., Pradhan, B. & Jamil, N.R. (2018). Relationship between design floods and land use land cover (LULC) changes in a tropical complex catchment. *Arabian Journal of Geosciences*, 11(14), p.376. https://doi.org/10.1007/s12517-018-3702-4.

AghaKouchak, A., Chiang, F., Huning, L. S., Love, C. A., Mallakpour, I., Mazdiyasni, O., ... & Sadegh, M. (2020). Climate extremes and compound hazards in a warming world. *Annual review of earth and planetary sciences*, 48(1), 519-548. https://doi.org/10.1146/annurev-earth-071719-055228.

Badan Nasional Penanggulangan Bencana (BNPB). (2025). *Bansor Sumatera 2025*. Retrieved from https://gis.bnpb.go.id/bansorsumatera2025/.

Basuki, T. M., Nugroho, H. Y. S. H., Indrajaya, Y., Pramono, I. B., Nugroho, N. P., Supangat, A. B., ... & Simarmata, D. P. (2022). Improvement of integrated watershed management in Indonesia for mitigation and adaptation to climate change: A review. *Sustainability*, 14(16), 9997. https://doi.org/10.3390/su14169997.

Bathurst, J. C., Bovolo, C. I., & Cisneros, F. (2010). Modelling the effect of forest cover on shallow landslides at the river basin scale. *Ecological Engineering*, 36(3), 317-327. https://doi.org/10.1016/j.ecoleng.2009.05.001.

Cao, Q., Liu, Y., Georgescu, M., & Wu, J. (2020). Impacts of landscape changes on local and regional climate: A systematic review. *Landscape Ecology*, 35(6), 1269-1290. https://doi.org/10.1007/s10980-020-01015-7.

Chen, L., Li, Y., & Cheng, Z. (2010). An overview of research and forecasting on rainfall associated with landfalling tropical cyclones. *Advances in Atmospheric Sciences*, 27(5), 967-976. https://doi.org/10.1007/s00376-010-8171-y.

Costa Alves, R. M., Neves Lousada, S. A., Cabezas, J., & Naranjo Gómez, J. M. (2023). Urban Flooding Risk in Machico and Planning Its Territory as a Form of Prevention. In S. Lousada (Ed.), *Geoinformatics in Support of Urban Politics and the Development of Civil Engineering* (pp. 50-76). IGI Global Scientific Publishing. https://doi.org/10.4018/978-1-6684-6449-6.ch003.

Cutter, S. L., Boruff, B. J., & Shirley, W. L. (2003). Social vulnerability to environmental hazards. *Social Science Quarterly*, 84(2), 242–261. https://doi.org/10.1111/1540-6237.8402002.

Daly, C., Conklin, D. R., & Unsworth, M. H. (2009). Local atmospheric decoupling in complex topography alters climate change impacts. *International Journal of Climatology*. 30 (12): 1857-1864. https://doi.org/10.1002/joc.2007.

Dimri, A. P. (2009). Impact of subgrid scale scheme on topography and landuse for better regional scale simulation of meteorological variables over the western Himalayas. *Climate dynamics*, 32(4), 565-574. https://doi.org/10.1007/s00382-008-0453-z.

Dolidon, N., Hofer, T., Jansky, L., & Sidle, R. (2009). Watershed and forest management for landslide risk reduction. *In Landslides–disaster risk reduction* (pp. 633-649). Berlin, Heidelberg: Springer Berlin Heidelberg. https://doi.org/10.1007/978-3-540-69970-5_33.

Golar, G., Muis, H., Isrun, I., Simorangkir, W. S., Fadhliah, F., Ali, M. N., & Basir-Cyio, M. (2024). Deforestation as a catalyst for natural disaster and community suffering: A cycle in the socioecological system. Folia Forestalia Polonica. *Series A. Forestry*, 66(2). https://doi.org/10.2478/ffp-2024-0007.

Gori, A., Lin, N. & Xi, D. (2020). Tropical cyclone compound flood hazard assessment: From investigating drivers to quantifying extreme water levels. *Earth's Future*, 8(12), p.e2020EF001660. https://doi.org/10.1029/2020EF001660.

Goyal, S., Mohapatra, M., Dube, S. K., Kumari, P., & De, I. (2016). Mesoscale convective systems in association with tropical cyclones over Bay of Bengal. *Natural Hazards*, 82(2), 963-979. https://doi.org/10.1007/s11069-016-2229-9.

Houze Jr, R. A. (2012). Orographic effects on precipitating clouds. *Reviews of Geophysics*, 50(1). https://doi.org/10.1029/2011RG000365.

Huang, C. Y., Chou, C. W., Chen, S. H., & Xie, J. H. (2020). Topographic rainfall of tropical cyclones past a mountain range as categorized by idealized simulations. *Weather and Forecasting*, 35(1), 25-49. https://doi.org/10.1175/WAF-D-19-0120.1.

Jothityangkoon, C., Hirunteeyakul, C., Boonrawd, K., & Sivapalan, M. (2013). Assessing the impact of climate and land use changes on extreme floods in a large tropical catchment. *Journal of Hydrology*, 490, 88-105. https://doi.org/10.1016/j.jhydrol.2013.03.036.

Mantero, G., Morresi, D., Marzano, R., Motta, R., Mladenoff, D. J., & Garbarino, M. (2020). The influence of land abandonment on forest disturbance regimes: a global review. *Landscape Ecology*, 35(12), 2723-2744. https://doi.org/10.1007/s10980-020-01147-w.

Nepal, S., Flügel, W. A., & Shrestha, A. B. (2014). Upstream-downstream linkages of hydrological processes in the Himalayan region. *Ecological Processes*, 3(1), 19. https://doi.org/10.1186/s13717-014-0019-4.

Silpamol, D. S., Kottayil, A., John, V. O., & Xavier, P. (2025). Characteristics of mesoscale convective systems during monsoon extreme rainfall events: case studies from the southwest coast of India. *Natural Hazards*, 121, 16897–16913 . https://doi.org/10.1007/s11069-025-07455-1.

United Nations Office for Disaster Risk Reduction (UNDRR). (2019). *Global assessment report on disaster risk reduction 2019*. UNDRR. eISBN: 978-92-1-004180-5

Van Vliet, M. T., Thorslund, J., Strokal, M., Hofstra, N., Flörke, M., Ehalt Macedo, H., ... & Mosley, L. M. (2023). Global river water quality under climate change and hydroclimatic extremes. *Nature Reviews Earth & Environment*, 4(10), 687-702. https://doi.org/10.1038/s43017-023-00472-3.

Widodo, T. N., Zubair, H., & Padjung, R. (2021). Land use change study and the increased risk of floods disaster in Jeneberang watershed at Gowa Regency, South Sulawesi, Indonesia. *In IOP Conference Series: Earth and Environmental Science* (Vol. 824, No. 1, p. 012045). IOP Publishing. https://doi.org/10.1088/1755-1315/824/1/012045.

Wisner, B., Blaikie, P., Cannon, T., & Davis, I. (2004). *At risk: Natural hazards, people's vulnerability and disasters (2nd ed.)*. Routledge. https://doi.org/10.4324/9780203428764.

Zscheischler, J., Westra, S., Van Den Hurk, B. J., Seneviratne, S. I., Ward, P. J., Pitman, A., ... & Zhang, X. (2018). Future climate risk from compound events. *Nature Climate Cchange*, 8(6), 469-477. https://doi.org/10.1038/s41558-018-0156-3.